

UCSF

UC San Francisco Previously Published Works

Title

High-resolution microarray analysis unravels complex Xq28 aberrations in patients and carriers affected by X-linked blue cone monochromacy

Permalink

<https://escholarship.org/uc/item/10w6f18g>

Journal

Clinical Genetics, 89(1)

ISSN

0009-9163

Authors

Yatsenko, SA
Bakos, HA
Vitullo, K
[et al.](#)

Publication Date

2016

DOI

10.1111/cge.12638

Peer reviewed



Published in final edited form as:

Clin Genet. 2016 January ; 89(1): 82–87. doi:10.1111/cge.12638.

High-resolution microarray analysis unravels complex Xq28 aberrations in patients and carriers affected by X-linked blue cone monochromacy

S.A. Yatsenko^{a,b,c}, H.A. Bakos^a, K. Vitullo^a, M. Kedrov^d, A. Kishore^b, B.J. Jennings^d, U. Surti^{a,b,c,e}, M.A. Wood-Trageser^b, S. Cercone^b, A.N. Yatsenko^{b,c}, A. Rajkovic^{a,b,c,e}, and A. Iannaccone^d

^aPittsburgh Cytogenetics Laboratory, Center for Medical Genetics and Genomics, Magee-Womens Hospital of UPMC, Pittsburgh, PA, USA

^bDepartment of Obstetrics, Gynecology and Reproductive Sciences, University of Tennessee Health Science Center, Memphis, TN, USA

^cDepartment of Pathology, University of Pittsburgh School of Medicine, Pittsburgh, PA, USA

^dDepartment of Ophthalmology, Hamilton Eye Institute, University of Tennessee Health Science Center, Memphis, TN, USA

^eDepartment of Human Genetics, Graduate School of Public Health, University of Pittsburgh, Pittsburgh, PA, USA

Abstract

The human X chromosome contains ~1600 genes, about 15% of which have been associated with a specific genetic condition, mainly affecting males. Blue cone monochromacy (BCM) is an X-linked condition caused by a loss-of-function of both the *OPNILW* and *OPNIMW* opsin genes. The cone opsin gene cluster is composed of 2–9 paralogs with 99.8% sequence homology and is susceptible to deletions, duplications, and mutations. Current diagnostic tests employ polymerase chain reaction (PCR)-based technologies; however, alterations remain undetermined in 10% of patients. Furthermore, carrier testing in females is limited or unavailable. High-resolution X chromosome-targeted CGH microarray was applied to test for rearrangements in males with BCM and female carriers from three unrelated families. Pathogenic alterations were revealed in all probands, characterized by sequencing of the breakpoint junctions and quantitative real-time PCR. In two families, we identified a novel founder mutation that consisted of a complex 3-kb deletion that embraced the *cis*-regulatory locus control region and insertion of an additional aberrant *OPNIMW* gene. The application of high-resolution X-chromosome microarray in clinical diagnosis brings significant advantages in detection of small aberrations that are beyond the

Corresponding author: Dr Svetlana A. Yatsenko, MD, Assistant Professor, Department of Obstetrics, Gynecology and Reproductive Sciences, University of Pittsburgh School of Medicine, UPMC, 300 Halket Street, Pittsburgh, PA 15213, USA. Tel.: +412 641 6693; fax: +412 641 2255; yatsenkosa@mail.magee.edu.

Supporting Information

Additional supporting information may be found in the online version of this article at the publisher's web-site.

Conflict of interest

The authors declare no conflict of interest.

resolution of clinically available aCGH analysis and which can improve molecular diagnosis of the known conditions and unravel previously unrecognized X-linked diseases.

Keywords

aCGH; blue cone monochromacy; color vision; X chromosome; X-linked disease; Xq28 deletion

A loss-of-function of both the *OPNILW* (red) and *OPNIMW* (green) cone opsin photopigment genes causes blue cone monochromacy (BCM; OMIM#303700), a rare X-linked, recessive disorder characterized by markedly reduced vision, severe photophobia, congenital nystagmus, and inability to discriminate colors. In humans, up to nine copies of the *OPNILW* and *OPNIMW* genes are arranged in a 5'–3' orientation within Xq28, forming the cluster (1–3). The close physical location and high (99.8%) sequence homology predispose this genomic region to non-allelic homologous recombination, which results in deletions, duplications, and the formation of *OPNILW/OPNIMW*-hybrid genes (4–6).

In the normal human retina, only the most proximal two genes in the cluster are expressed (2). Red or green expression in cone photoreceptors is accomplished by interaction of the gene promoter with a locus control region (LCR), a unique *cis*-regulatory DNA sequence located ~4 kb upstream of *OPNILW* (7). In about 90% of males affected by BCM, Xq28 deletions or point mutations inactivating both *OPNILW* and *OPNIMW* have been identified by polymerase chain reaction (PCR)-based molecular testing, while ~10% of patients have negative results and the molecular defects remain unknown (2, 6), precluding accurate information on disease progression in affected males and female carriers, carrier and prenatal testing, potential approaches, and efficiency of gene therapy. The Xq28 deletions may remove the LCR, inactivating both wild-type opsin genes, or extend into the opsin cluster (4, 6). The complex structure of the LCR and opsin genes, the presence of highly homologous sequences, and variability within the opsin genomic region among human populations pose multiple challenges and limit the effectiveness of diagnostic and carrier testing in families with BCM.

Microarray platforms are now used extensively for diagnosis and research to detect genomic imbalances contributing to human disease and population diversity (8, 9). High-resolution microarrays provide distinct benefits in studying males affected with X-linked disorders (9). Single gene alterations are more likely to be present in affected males; however, the resolution of clinical whole-genome microarray platforms, ranging from 25–200 kb, is often insufficient to detect smaller X-chromosome imbalances. We identified novel molecular alterations in three BCM families, using high-resolution X chromosome-targeted (X-HR) array comparative genomic hybridization (aCGH) and report the advantages and limitations of microarray analysis in the diagnosis of BCM and other X-linked conditions.

Materials and methods

Subjects

Three unrelated men (P1–P3; Fig. 1) with a clinical diagnosis of BCM (10) were referred for testing by X-HR microarray. Informed consents were obtained using the UTHSC IRB

protocols. Control samples from 268 women and 42 de-identified males who underwent microarray clinical testing unrelated to BCM condition were recruited under the University of Pittsburgh IRB guidelines.

X-HR microarray design

We developed a custom oligonucleotide microarray using a 4×180K CGH platform (Agilent, Santa Clara, CA). The X-HR microarray consists of 166,000 oligonucleotide probes, covering the X chromosome with an average 1 probe/kb, and an enhanced (1 probe/200–500 bp or 10 probes/gene) coverage of all X-linked genes. This microarray has been validated on samples with X-chromosome imbalances and implemented for clinical diagnostic testing.

Array-CGH studies

The X-HR microarray studies were performed on male patients P1–P3 and female carriers (Family-1 III-4, Family-2 IV-11 and IV-13). DNA samples from 42 males hybridized vs male reference (Coriell, NA12891), 10 males hybridized against Agilent male reference, and 268 females hybridized against female reference (Promega, G152) not affected by BCM were analyzed by X-HR, serving as a negative control, and were also used to calculate the frequency of opsin gene copy number in a normal population. A whole-genome 180 K CGH + SNP microarray (ISCA design, Agilent) was performed on the brother of P1 (Family-1 IV-3). See Appendix S1, Supporting Information.

Quantitative real-time PCR

To determine the total number of red and green opsin genes, qPCR using iQ-SYBR Green Supermix (Bio-Rad Laboratories, Hercules, CA) was performed on P2 and the reference DNA (Appendix S1).

Results

Microarray studies in BCM families

In P1, X-HR microarray detected a hemizygous loss (chrX:153,405,331–153,406,875; hg19) encompassing an at least 1.5-kb segment (Fig. 2a), with the proximal breakpoint within the chrX:153,403,612–153,405,331 interval, and the distal breakpoint within the chrX:153,406,875–153,409,337 segment, indicating a deletion ranging from 1.544 kb (minimum) to 6.126 kb (maximum). This deletion includes the LCR (Fig. 2e). In addition, X-HR showed a gain suggestive of an extra opsin gene copy in the patient as compared to the reference DNA. Identical, but heterozygous deletion ($\log_2(1/2) = -1.0$) was detected in the patient's mother (Fig. 2b). In the brother (IV-3; Fig. 1), a whole-genome microarray identified a *de novo* 9.3-Mb gain in the 4p16.1-pter region (Fig. S2a), which probably explains his intellectual disability, but did not detect alterations in Xq28. Visual examination of the aCGH plot revealed insufficient coverage within the opsin gene cluster (Fig. S2b).

In P2, X-HR analysis revealed a loss ($\log_2(2/3) = -1.58$) in Xq28 (chrX:153,416,333–153,459,120), consistent with a deletion of at least two of three copies of the opsin genes (Fig. 2c), with the proximal breakpoint in chrX:153,414,302–153,416,333 (*OPNILW* intron

1) and the distal breakpoint downstream of *OPNIMW* exon 6 (Fig. 2e), probably altering structure or function of the third opsin gene in the cluster. See Appendix S1 for qPCR confirmation. Two daughters (Family-2 IV-11 and IV-13; Fig. 1) showed the same Xq28 alteration (Fig. 2d).

In P3, X-HR microarray detected a loss involving the LCR and a gain in the opsin gene cluster region, identical to those of patient P1 (Fig. 2a). Comparison of the benign copy number variants along the X chromosome between P1 and P3 showed no similarity, thus excluding a close relationship between these two patients. Deletions detected in the affected males were absent in the 268 female and 42 male control samples.

Breakpoint junction analysis

We further analyzed breakpoints in individuals from Families 1 and 3. Primers p1F1 and p1R1, mapped to the proximal and the distal sequences flanking the LCR deletion, were designed to amplify the breakpoint junction and a 6234-bp wild-type fragment (Table S1). Long-range PCR was performed on DNA from a control (wt) female and male, P1, his affected brother (F1 IV3) and mother (F1 III4), and P3. PCR yielded two abnormal fragments (~4 kb and 2.7 kb) in the affected males and the carrier mother (Fig. 3a,b), consistent with the Xq28 deletion detected by aCGH. Neither junction was observed using the same PCR primers to amplify the genomic male and female reference DNA.

Direct sequencing of the patient-specific products revealed a complex rearrangement upstream of the *OPNILW* gene. This aberration, identical in P1 and P3, included a 2991-bp deletion embracing the entire LCR, insertion of an extra copy of the green-pigment gene (*OPNIMW*), and a tandem duplication of a 1345-bp sequence encompassing the promoter, exon 1, and a part of *OPNIMW* intron 1 (Fig. 3c,d). The deletion–insertion breakpoints were located within two *Alu* elements, *AluSx* and *AluSx1*, oriented in the same direction, with ~79% homology between them (Fig. 3d). The junction occurred in a 16-bp microhomology segment (AGAGGTTGT/CAGTGAGC) (Fig. S3). The structure of an extra (inserted) *OPNIMW* gene is altered by a duplication of the 1345 bp sequence. The duplicated DNA segment comprises exon 1; therefore, two mutant PCR fragments were obtained in P1 and P3 using the p1F1 and p1R1 primers. The duplication junction occurred between non-homologous sequences. Comparison of the single nucleotide polymorphisms (SNPs) in the unique sequence revealed that P1 and P3 exhibit the same haplotype; therefore, the complex rearrangement probably represents a founder mutation.

Discussion

Historically, X-linked recessive disorders were studied by PCR-based molecular methods due to their higher resolution compared to cytogenetic techniques. Despite its wide use in clinical diagnosis, PCR amplification of repetitive and rearranged DNA segments is highly problematic as it requires prior target sequence information and cannot test for duplications. Furthermore, the precise breakpoints of a deletion are difficult to determine; thus, testing for female carriers by this method is of very limited utility. In contrast to targeted approaches, microarray-based techniques have enabled detection of individual genomic variations, such as deletions, duplications, and amplifications, at a very high resolution in both males and

females regardless of prior knowledge of the region of interest (8, 9). We applied a high-resolution microarray that can detect X-chromosome imbalances with at least 10-fold higher resolution than the clinical 180 K CGH+SNP array to study males and carrier females affected by BCM as well as a population of unaffected female and male controls (Figs S4–S7).

It is not surprising that previous PCR-based testing was unsuccessful in these families, taking into consideration the complexity of the rearrangement and the peculiar structure of the cone opsin gene cluster (1, 5–7). Interstitial chromosomal rearrangements are frequently mediated by recombination between flanking segmental duplications (11); however, analysis of repetitive sequences is itself challenging. Duplicated regions of the genome usually represent a cluster of structurally and functionally related genes (paralogs) and pseudogenes with a high degree of sequence homology (11, 12). Such regions are ‘hot spots’ for non-homologous and intragenic recombination or gene conversion rearrangements that can lead to pathogenic alterations as well as to genetic diversity among healthy individuals (5, 11, 12).

Indeed, intragenic recombination between normal functional gene copies leads to the production of hybrid red/green-cone genes (3, 4). About 70% of males carry three copies of the cone opsin photopigment gene on the X chromosome (3). Gains in copy number within the cone opsin gene cluster are observed in 10–15% of men and are considered to be benign copy number variants. Normal function of red- and green-pigment opsin genes strongly depends on the specific arrangements of gene coding and *cis*-regulatory sequences in the cluster. In males with normal color vision, additional hybrid red/green-cone genes must be positioned more distally to the functional copies on the X chromosome (1–4).

Up to 10% of males have red or green color vision deficiency as the result of displacement or replacement of the normal functional *OPNILW* or *OPNIMW* gene by a hybrid copy. Analysis of the junction fragments in P1 and P3 showed that the insertion of an additional green opsin gene copy took place at the first, most proximal, position in the cluster. In addition, this also resulted in ~3-kb deletion of the regulatory region, resulting in BCM.

Interestingly, deletion–insertion junction breakpoints were located within the 16-bp microhomology segments of two *Alu* elements, suggestive of a microhomology-mediated break-induced replication (MMBIR) mechanism (12). Complex aberration in both P1 and P3 is consistent with a founder mutation; however, genomic instability in the opsin cluster region and the presence of *Alu* repetitive sequences with extended segments of microhomology may result in sporadic reoccurrence of similar mutations. Both of our patients also have a 1.3-kb duplication, and it is possible that the insertion–deletion–duplication rearrangement occurred simultaneously. Alternatively, the exon 1 duplication may have arisen independently from the insertion–deletion rearrangement, or it may exist as a hybrid gene polymorphism within a population.

The high-density X-HR microarray was invaluable in identifying novel deletions and duplications in the studied families. In contrast to other clinical microarray platforms that do not usually contain probes for segmental duplicons, we were able to analyze copy number

variations in paralogous gene clusters and therefore detected a pathogenic deletion in P2. BCM is considered to be a stationary disorder; however, the recent studies showed the correlation of a specific molecular defect with clinical manifestations and disease progression. Moreover, female carriers may present with some degree of retinal degeneration or progressive vision loss (13, 14). Carrier testing in females depends on the molecular findings in the affected males and is commonly problematic. This highlights the importance of establishing more reliable approaches for the discovery of underlying molecular defects for X-linked conditions. Incorporation of high-resolution X-chromosome microarray testing into the routine clinical diagnosis in conjunction with mutation analysis can improve molecular diagnosis for known conditions and unravel previously unrecognized X-linked diseases.

Supplementary Material

Refer to Web version on PubMed Central for supplementary material.

Acknowledgments

We thank the families for participating in this study. We are grateful to Bruce Campbell, scientific editor at the Magee-Womens Research Institute (MWRI), for the editing and useful comments. This work was supported by the National Institute of Child Health and Human Development (R21HD074278, A. R.) and the MWRI Postdoctoral Fellowship (MA. W.-T.).

References

1. Vollrath D, Nathans J, Davis RW. Tandem array of human visual pigment genes at Xq28. *Science*. 1988; 240:1669–1672. [PubMed: 2837827]
2. Hayashi T, Motulsky AG, Deeb SS. Position of a ‘green-red’ hybrid gene in the visual pigment array determines colour-vision phenotype. *Nat Genet*. 1999; 22:90–93. [PubMed: 10319869]
3. Drummond-Borg M, Deeb SS, Motulsky AG. Molecular patterns of X chromosome-linked color vision genes among 134 men of European ancestry. *Proc Natl Acad Sci U S A*. 1989; 86:983–987. [PubMed: 2915991]
4. Neitz J, Neitz M. The genetics of normal and defective color vision. *Vision Res*. 2011; 51:633–651. [PubMed: 21167193]
5. Reyniers E, Van Thienen MN, Meire F, et al. Gene conversion between red and defective green opsin gene in blue cone monochromacy. *Genomics*. 1995; 29:323–328. [PubMed: 8666378]
6. Gardner JC, Webb TR, Kanuga N, et al. X-linked cone dystrophy caused by mutation of the red and green cone opsins. *Am J Hum Genet*. 2010; 87:26–39. [PubMed: 20579627]
7. Wang Y, Macke JP, Merbs SL, et al. A locus control region adjacent to the human red and green visual pigment genes. *Neuron*. 1992; 9:429–440. [PubMed: 1524826]
8. Lee C, Iafrate AJ, Brothman AR. Copy number variations and clinical cytogenetic diagnosis of constitutional disorders. *Nat Genet*. 2007; 39:S48–S54. [PubMed: 17597782]
9. Hegde MR, Chin EL, Mülle JG, Okou DT, Warren ST, Zwick ME. Microarray-based mutation detection in the dystrophin gene. *Hum Mutat*. 2008; 29:1091–1099. [PubMed: 18663755]
10. Luo X, Cideciyan AV, Iannaccone A, et al. Blue cone monochromacy: visual function and efficacy outcome measures for clinical trials. *PLoS One*. 2015; 10:e0125700. [PubMed: 25909963]
11. Lupski JR. Genomic rearrangements and sporadic disease. *Nat Genet*. 2007; 39:S43–S47. [PubMed: 17597781]
12. Hastings PJ, Ira G, Lupski JR. A microhomology-mediated break-induced replication model for the origin of human copy number variation. *PLoS Genet*. 2009; 5:e1000327. [PubMed: 19180184]

13. Gardner JC, Michaelides M, Holder GE, et al. Blue cone monochromacy: causative mutations and associated phenotypes. *Mol Vis.* 2009; 15:876–884. [PubMed: 19421413]
14. Carroll J, Rossi EA, Porter J, et al. Deletion of the X-linked opsin gene array locus control region (LCR) results in disruption of the cone mosaic. *Vision Res.* 2010; 50:1989–1999. [PubMed: 20638402]

Author Manuscript

Author Manuscript

Author Manuscript

Author Manuscript

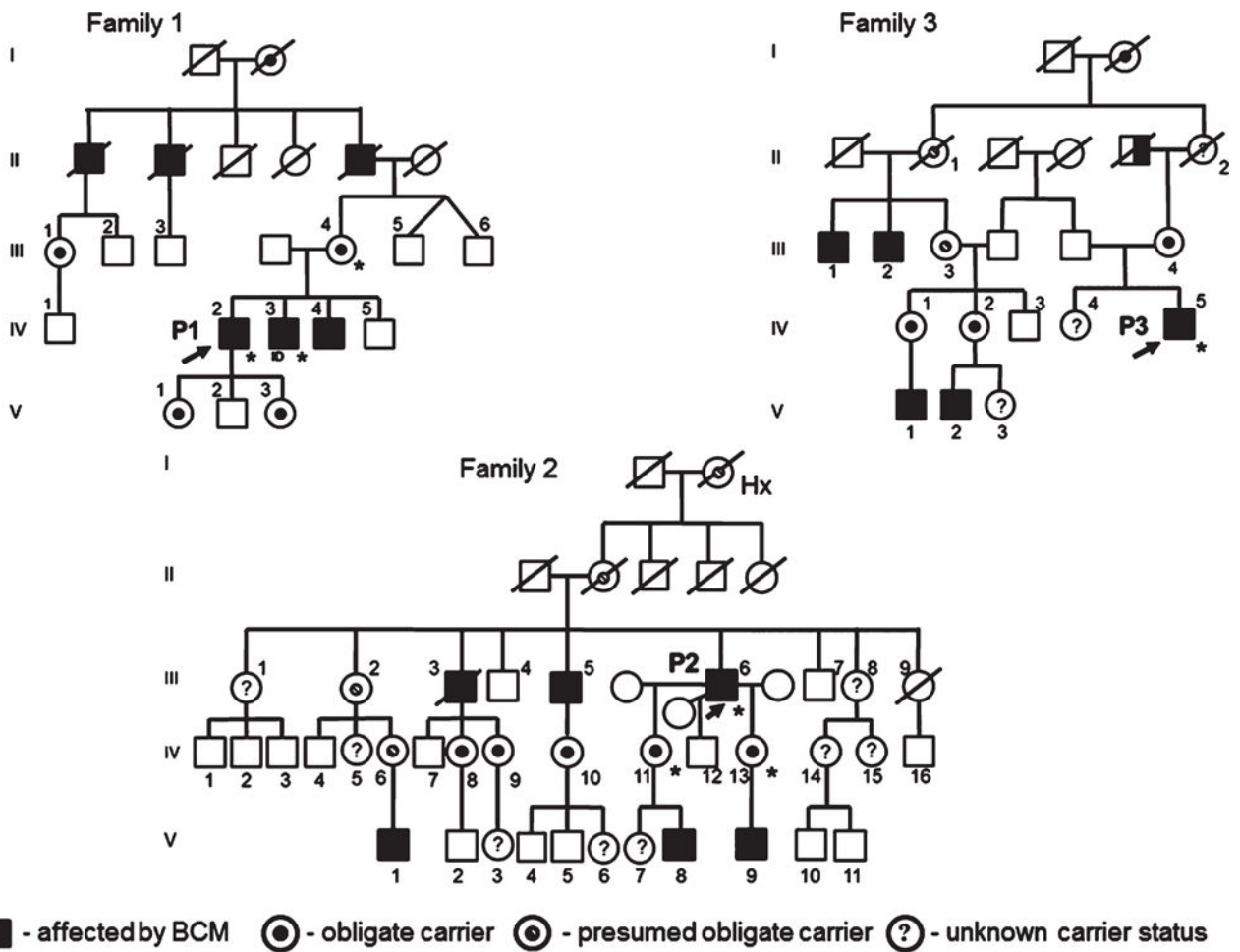


Fig. 1. Five-generation pedigrees. Black squares represent affected males with blue cone monochromacy (BCM). Retinal findings of these three subjects were reported previously (10) and are summarized in the Appendix S1. Slashes through symbols indicate deceased individuals; the arrows designate the probands P1, P2, and P3 in Families 1, 2, and 3, respectively. Hx, family history of vision problems among relatives on the grandmother's side of the proband P2. The maternal grandfather of the proband P3 (half-filled square) – affected by hearsay; ID, brother (Family 1, IV-3) of the proband P1 with intellectual disability and BCM; *, confirmed deletion in Xq28. Previous molecular studies at another institution performed on all affected individuals (P1, P2, and P3) by multiple ligation-dependent probe amplification (MPLA) assay did not detect Xq28 deletions.

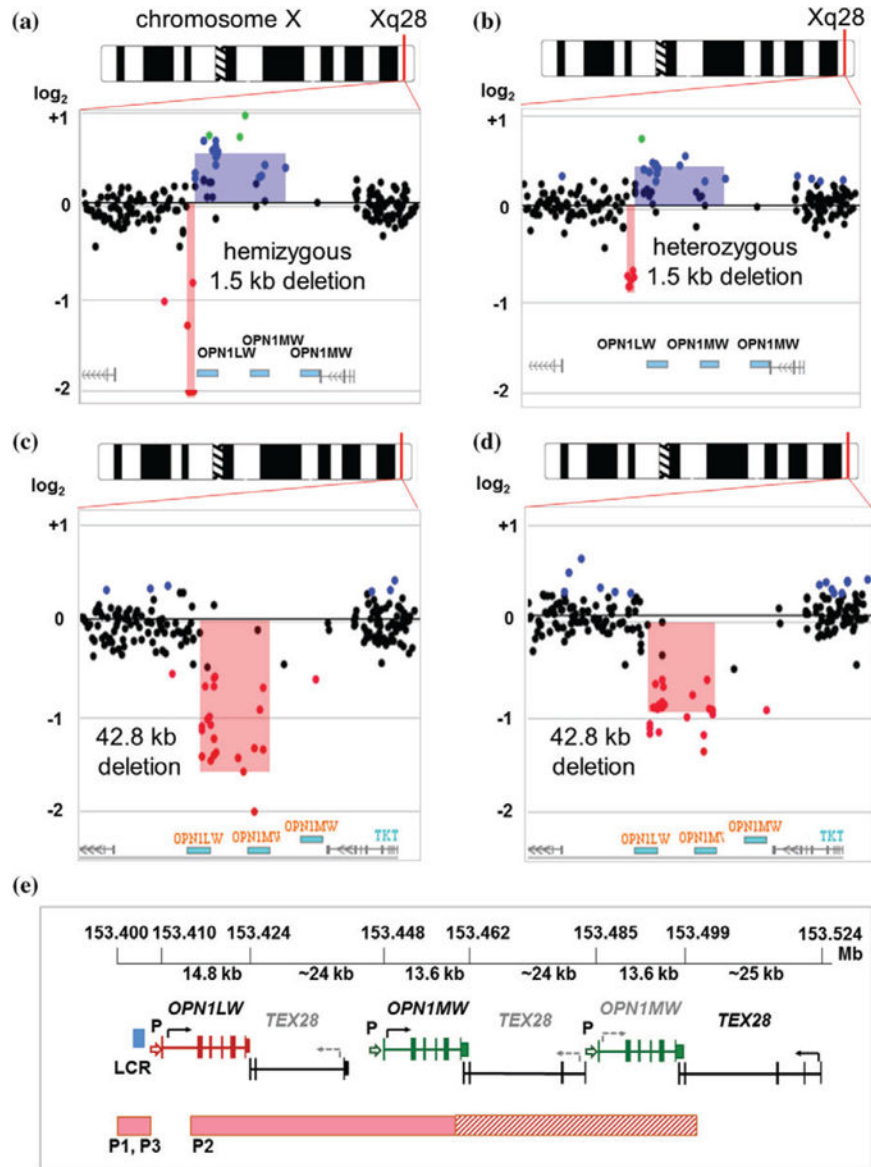
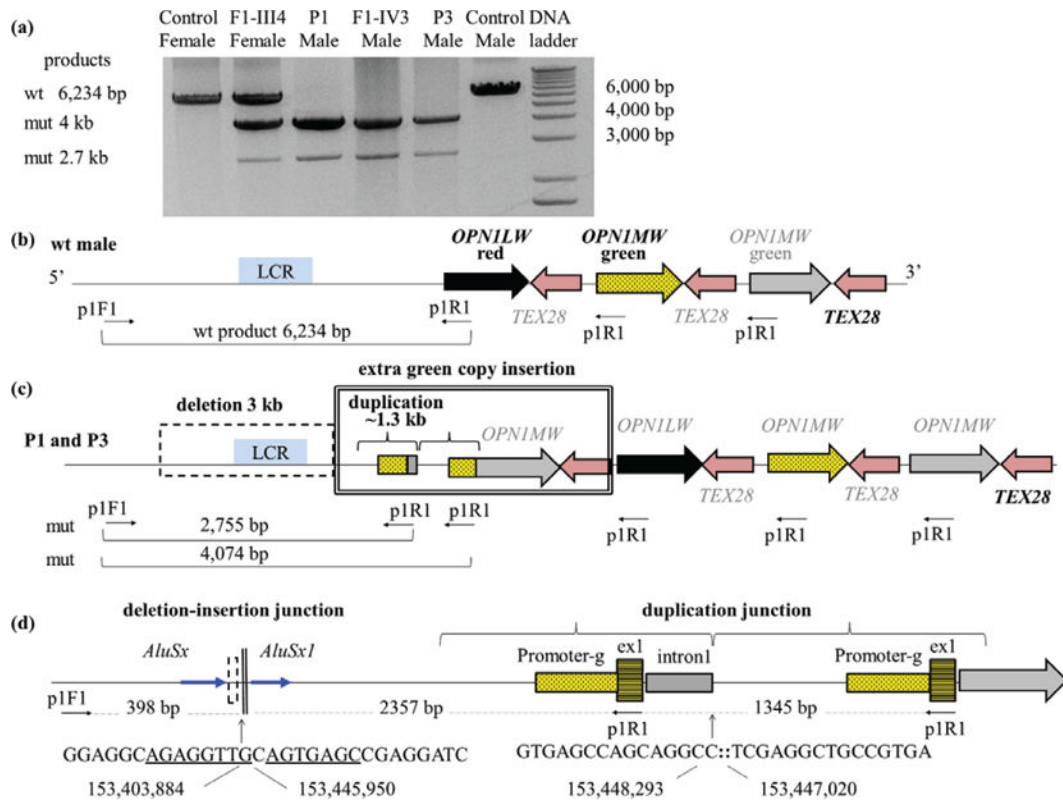


Fig. 2. The Xq28 deletions detected by X-HR microarray. **(a)** An array-CGH plot showing copy number alterations in the Xq28 region in the male patient P1 (Family 1, IV-2) and **(b)** his mother (Family 1, III-4). Top, an idiogram of the X chromosome. The Xq28 region is indicated by a red line. Below, a magnified view of the Xq28 region showing a loss (pink shaded area) upstream of the *OPN1LW* gene and a gain (blue shaded area) in the total number of opsin genes. On the array-CGH plot, each dot represents an oligonucleotide DNA probe, arranged according to genomic location, from the proximal (left) to the distal long arm (right) of the X chromosome. The fluorescence intensity ratio Cy5/Cy3 (test/reference signal) for each probe is displayed as a logarithmic (\log_2) value on the Y-axis. Black dots represent probes with no change in DNA copy number (\log_2 above -0.5 and less than $+0.2$). Red dots indicate a loss in DNA copy number ($\log_2 < -0.5$). Gain in DNA copy number is detected for the segments with an average $\log_2 > +0.2$ (blue dots). In the proband P1 **(a)**, an

average \log_2 of < -2.0 indicates a hemizygous deletion ($\log_2(0/1) = -\infty$) upstream of the *OPNILW* gene. **(c)** X-HR microarray plot showing a loss (pink shaded area) of an at least 42.8 kb segment in the proband P2 (Family 2, III-6), and **(d)** his daughter (Family 2, IV-11). **(e)** A schematic representation of the human opsin gene cluster region. Top, genomic location (chrX:153.400–153.525 Mb; hg19) of the cluster, size, and distance between the opsin genes is shown. The single red opsin gene (14.8 kb in size) and the adjacent green opsin gene (13.6 kb) are expressed. Functional copies of the genes are indicated by bold font (black arrows indicate the direction of transcription). Inactive copies are marked by gray font (gray dashed arrows indicate the 5'–3' direction of an inactive gene). Each *OPNILW* and *OPNIMW* consists of six exons, indicated by vertical bars, separated by the *TEX28* genes. 'P' indicates a promoter sequence. Locus control region (LCR) is shown as a blue box. Deletions in the probands P1, P2, and P3 are shown by horizontal pink bars. In P2, the exact position of the distal breakpoint could not be precisely determined due to the repetitive structure of the DNA sequences in that region. Hatched bar indicates region of uncertainty for P2.

**Fig. 3.**

Breakpoint junctions in Families 1 and 3. (a) Two patient-specific junction fragments (mut) of ~2.7 kb and 4 kb were obtained from the affected male patients and the mother of P1 (Family 1, III-4). Amplification of the male and female reference DNA yielded a single 6.2-kb (wt) band. (b) Structure of the opsin cluster in a normal wild-type (wt) male. Gray arrowhead indicates a non-functional (green or hybrid) copy. Primers p1F1 and p1R1 were used to amplify a wt fragment. Primer p1F1 is mapped within the unique Xq28 sequence upstream of locus control region (LCR; blue box). Reverse primer p1R1 is located within the exon 1, which is identical in *OPNILW* and *OPNIMW*. (c) A complex rearrangement in P1 and P3. A total of four opsin genes are present. Dotted rectangle indicates a deletion encompassing the LCR. An additional copy of a green opsin gene is inserted upstream of the red pigment gene (depicted by a double-line rectangle). The structure of an inserted *OPNIMW* gene is altered by a duplication of a 1345-bp sequence, containing exon 1. (d) Direct sequence analysis of the mutant junction fragments from probands P1 and P3. The deletion–insertion junction (dashed box/double-line structure) is shown on the left. ‘Promoter-g’ designates *OPNIMW* promoter. *Alu* sequences are indicated by blue arrows. Duplication junction occurs between intron 1 and sequence located upstream of the green promoter. Below, the sequences of the junction fragments and genomic coordinates are given. Underlined nucleotides indicate microhomology at the breakpoint junction.